Shock Waves
DOI 10.1007/s00193-017-0733-9

ORIGINAL ARTICLE

Full-scale testing of leakage of blast waves inside a partially vented room exposed to external air blast loading

R. Codina[1,2] · **D. Ambrosini**[1,2]

Received: 26 December 2016 / Revised: 2 June 2017 / Accepted: 6 June 2017

Abstract For the last few decades, the effects of blast loading on structures have been studied by many researchers around the world. Explosions can be caused by events such as industrial accidents, military conflicts or terrorist attacks. Urban centers have been prone to various threats including car bombs, suicide attacks, and improvised explosive devices. Partially vented constructions subjected to external blast loading represent an important topic in protective engineering. The assessment of blast survivability inside structures and the development of design provisions with respect to internal elements require the study of the propagation and leakage of blast waves inside buildings. In this paper, full-scale tests are performed to study the effects of the leakage of blast waves inside a partially vented room that is subjected to different external blast loadings. The results obtained may be useful for proving the validity of different methods of calculation, both empirical and numerical. Moreover, the experimental results are compared with those computed using the empirical curves of the US Defense report/manual UFC 3-340. Finally, results of the dynamic response of the front masonry wall are presented in terms of accelerations and an iso-damage diagram.

Keywords Leakage of blast waves · External blast loading · Vented room · Confinement · Internal overpressures and impulses · Masonry wall

Communicated by D. Frost.

✉ D. Ambrosini
dambrosini@uncu.edu.ar

[1] Structural Engineering Master Program, Engineering Faculty, University of Cuyo, Mendoza, Argentina

[2] CONICET, National Research Council from Argentina, Buenos Aires, Argentina

1 Introduction

For the last few decades, the effects of blast loading on structures have been studied by many researchers around the world. The explosions can be caused by events such as industrial accidents, military conflicts or terrorist attacks. Urban centers have been prone to various threats including car bombs, suicide attacks, and improvised explosive devices (IEDs). Therefore, the study of blast waves in urban environments is important to develop blast mitigation strategies, protection systems [1], and for post-blast forensic investigations [2].

For the first 60 years of the twentieth century, various criteria and methods based upon results of catastrophic events together with empirical formulas and charts were used for the design of explosive facilities. Simplified analytical models and empirical methods, such as those found in technical manuals like UFC 3-340-02 [3] and TM5-855-1 [4], or software such as CONWEP [5], were used to solve this kind of problem. Some of these methods can be found in classical books like Baker et al. [6], Smith and Hetherington [7], and Cormie et al. [8]. For simple geometries and open spaces, simple tools may be acceptable. However, for actual, complex cityscapes, reasonably accurate prediction of blast effects will, in general, require numerical simulations validated against experimental observations. The effects associated with façades of buildings subjected to blast loading were studied by Smith et al. [9] and the clearing effects in finite targets by Tyas et al. [10] using experimental models and semi-empirical functions.

Urban environments present obstructions for blast waves, producing multiple reflections which can have a significant effect on the resulting blast loading on buildings in the path of the blast wave [11]. Numerical simulations of blast loading in urban environments using an overset meshing strategy were

Published online: 23 June 2017

Fig. 1 Room for experimental tests

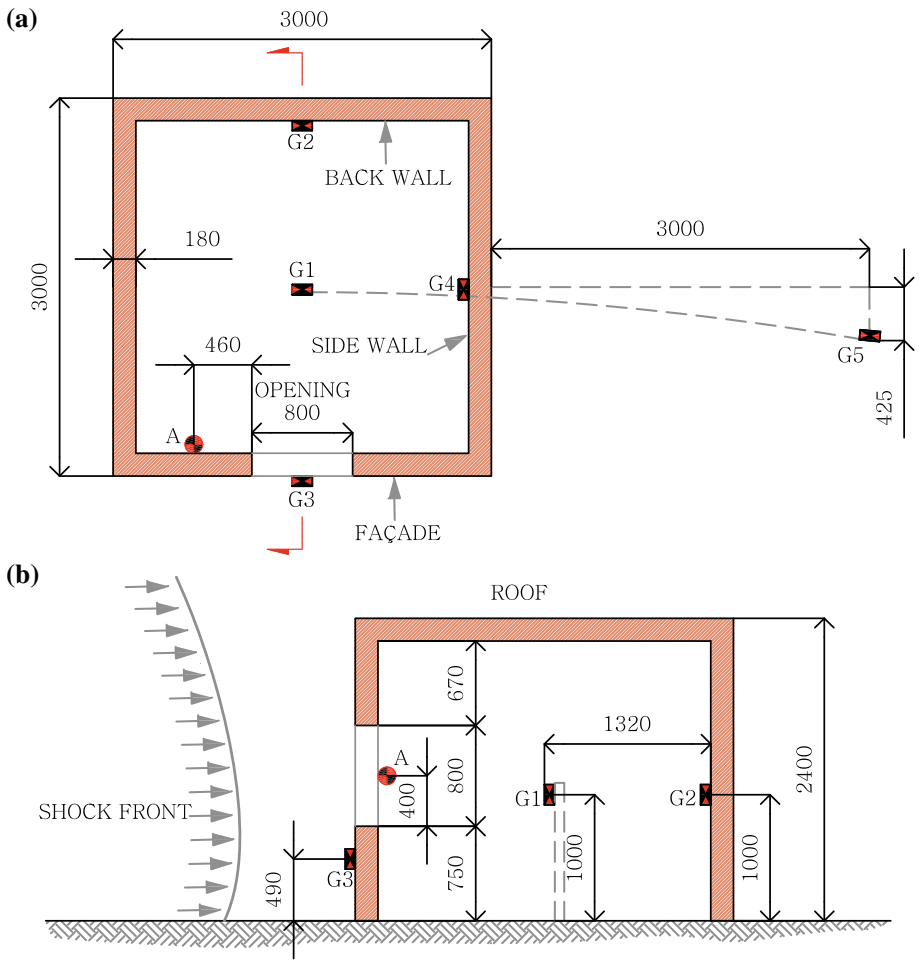

Fig. 2 Location of sensors (distances in mm). **a** Plan view. **b** Section view

Table 1 Properties of Gelamón VF65 (www.fm.gob.ar)

Density g/cm^3	Velocity of detonation m/s	Pressure of detonation MPa	Volume of gases m^3/kg	Relative effectiveness factor
1.5	6000	13,950	0.682	0.65

Table 2 Test setup

Test	Charge eq. TNT W (kg TNT)	Standoff distance R (m)	Scaled distance $Z = \frac{R}{\sqrt[3]{W}}$ (m/kg$^{1/3}$)	Angle α (°)
1	1	15.00	15.0	0
2	5	25.00	14.6	0
3	5	28.86	16.8	30
4	5	25.00	14.6	0

presented by Wang et al. [11]. On the other hand, Rose et al. [12] studied the interaction of oblique blast waves with buildings.

Remennikov and Rose [13] presented the results of CFD calculations to determine building blast loads for complex city geometries. The behavior of air blast waves in complex geometries like cities was investigated by Smith and Rose [14], who showed that shielding and channeling effects must be considered in urban city streets. Shock interaction with buildings in combination with a damage criterion was studied by Luccioni et al. [15]. Gebbeken and Döge [16] investigated the effects of different façade geometries on blast-induced loads. Finally, Codina et al. [17] studied channeling effects for different street widths, amounts and location of explosive loads, obtaining maps of overpressure and impulse amplification.

Structures can be subjected to internal or external blast loads. In the first case, explosions may occur due to various reasons, e.g., as a result of an ammunition storage explosion, a charge explosion within a room in a terrorist action, or a warhead explosion following its penetration into a closed space [18]. A confined explosion causes more damage than a similar external free-field explosion. Typical time histories of overpressures acting on the wall of vented and fully confined structures are shown in Anderson et al. [19]. Internal blast loads exhibit two phases. In the first, the reflected blast load consists of an initial high-pressure, short-duration reflected wave, followed by several reflected shocks. The second phase is characterized by a slowly decaying pressure. A full-scale experimental study aiming at understanding some characteristics of an interior explosion within a room with no venting or with limited venting has been carried out by Edri et al. [20]. Feldgun et al. [18] presented a thermodynamic model for the prediction of the residual gas pressure including afterburning energy release. Sauvan et al. [21] reported the blast wave interactions that resulted from the detonation of a stoichiometric propane–oxygen mixture in a confined room.

Partially vented constructions subjected to an external blast loading are also an important topic in protective engineering. When a shock front strikes the front wall of a structure, the windows and doors will, in general, fail after the impact of the shock front unless they were designed to resist the applied loads. Consequently, blast pressures will flow into the structure through these openings. The waves from leakage are weaker than the incident pressure at the building exterior. However, the interior overpressure may be of

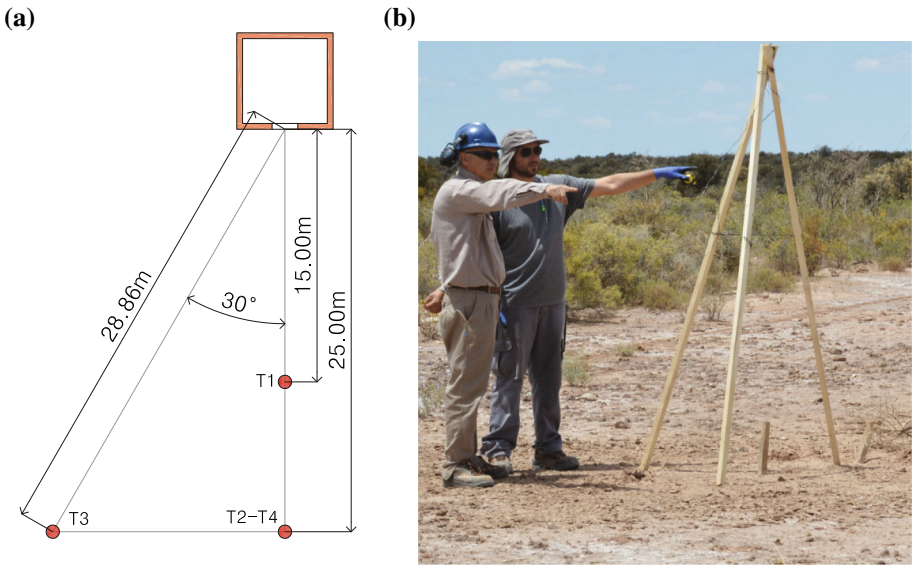

Fig. 3 Test setup. **a** Explosive location scheme. **b** Tripod to suspend the explosive charge

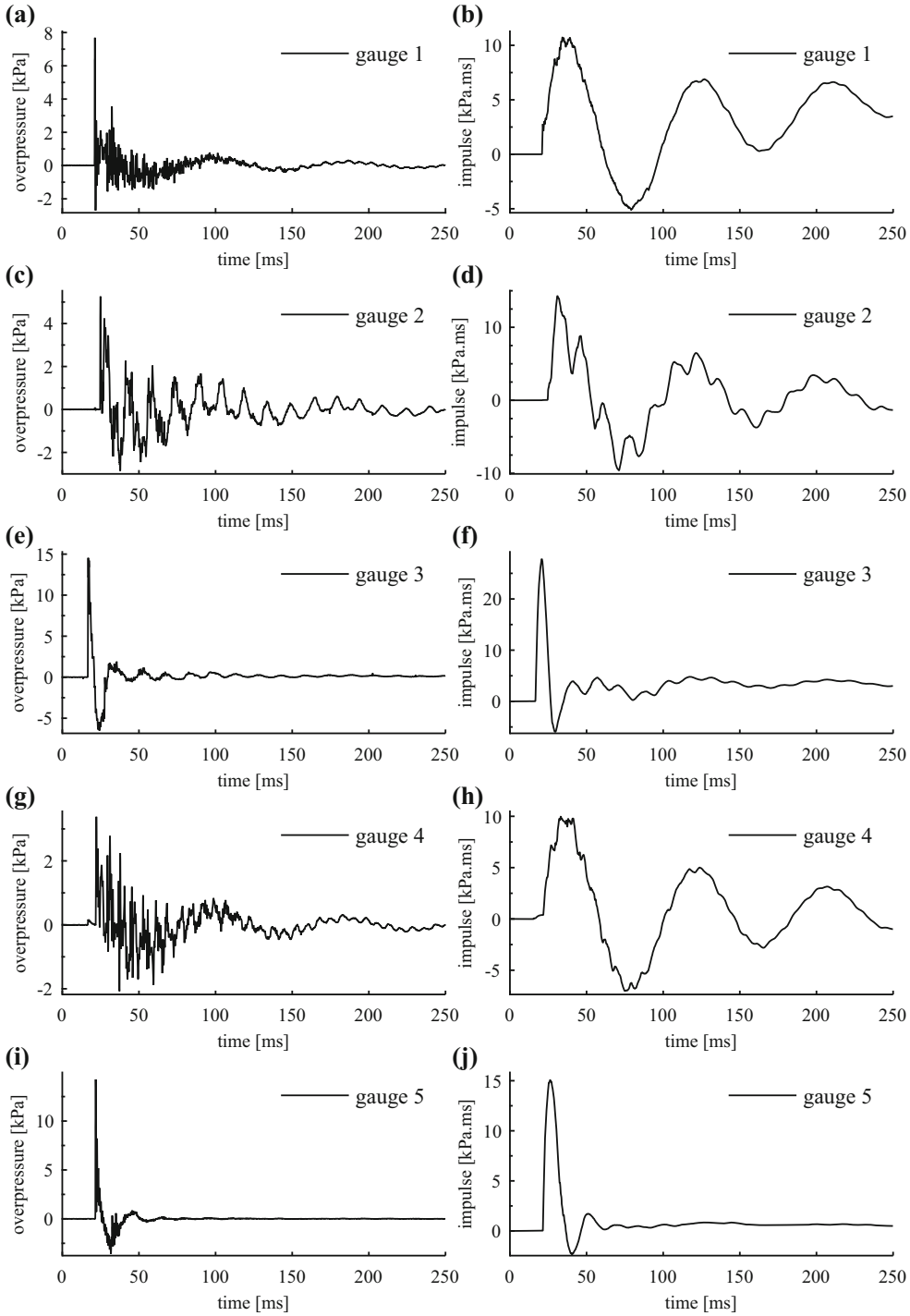

Fig. 4 Overpressure and impulse time history for test 1. **a**, **b** Center of the room. **c**, **d** Back wall. **e**, **f** Façade. **g**, **h** Side wall. **i**, **j** Exterior gauge

sufficient magnitude to cause damage due to multiple reflections with the interior building walls and other components. The study of the leakage of the waves is necessary to assess blast survivability inside structures. Another important task in protective engineering is to make a realistic prediction of internal blast pressures to develop design provisions with respect to internal elements like partitions, hung ceilings, lighting fixtures, equipment, mechanical and electrical fixtures, piping, and conduits. These elements may be prone to being dislodged as a result of structural motions or overpressures and become a hazard to the building's occupants and contents, UFC 3-340-02 [3]. The literature regarding the estimation of overpressures inside buildings due to external blast loadings is very limited. Ram et al. [22] used scaled-

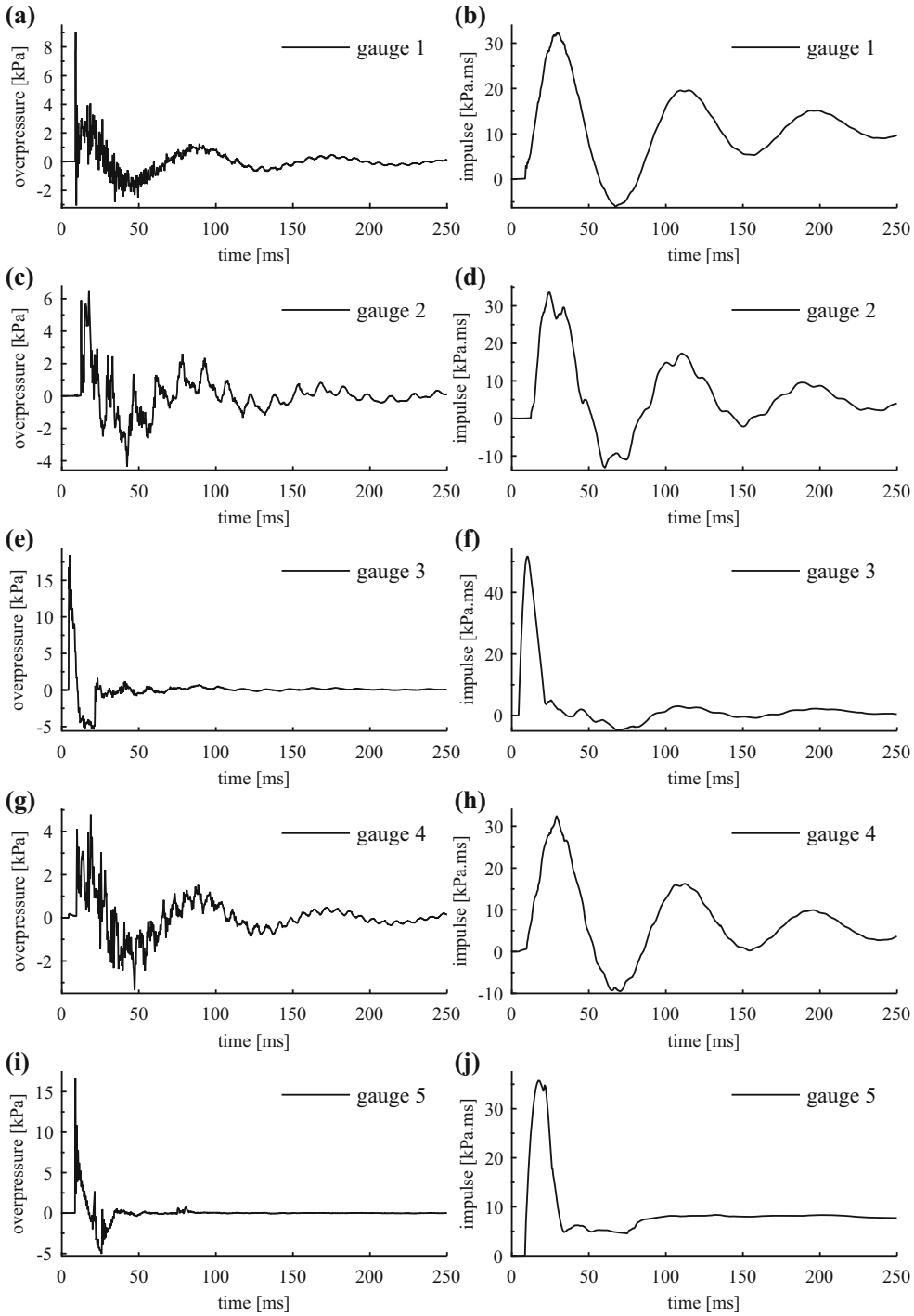

Fig. 5 Overpressure and impulse time history for test 2. **a**, **b** Center of the room. **c**, **d** Back wall. **e**, **f** Façade. **g**, **h** Side wall. **i**, **j** Exterior gauge

down models to investigate how the pressure and impulse imposed at the frontal façade of a structure together with the internal structural geometry affect the developing load on the target wall inside the structure. Results show that the peak impulse recorded at the target wall is independent of internal geometry. The effects of overpressure inside buildings due to external blast loading were illustrated by Luccioni et al. [23] in the case of the AMIA building. In this case, the overpressures produced progressive collapse of the building.

In the present paper, a partially vented room is subjected to different external blast loadings. Full-scale tests are performed to study the effects of the leakage of the blast waves inside the structure. The results obtained may be useful for proving the validity of different methods of calculation, both empirical and numerical. Moreover, the experimental results

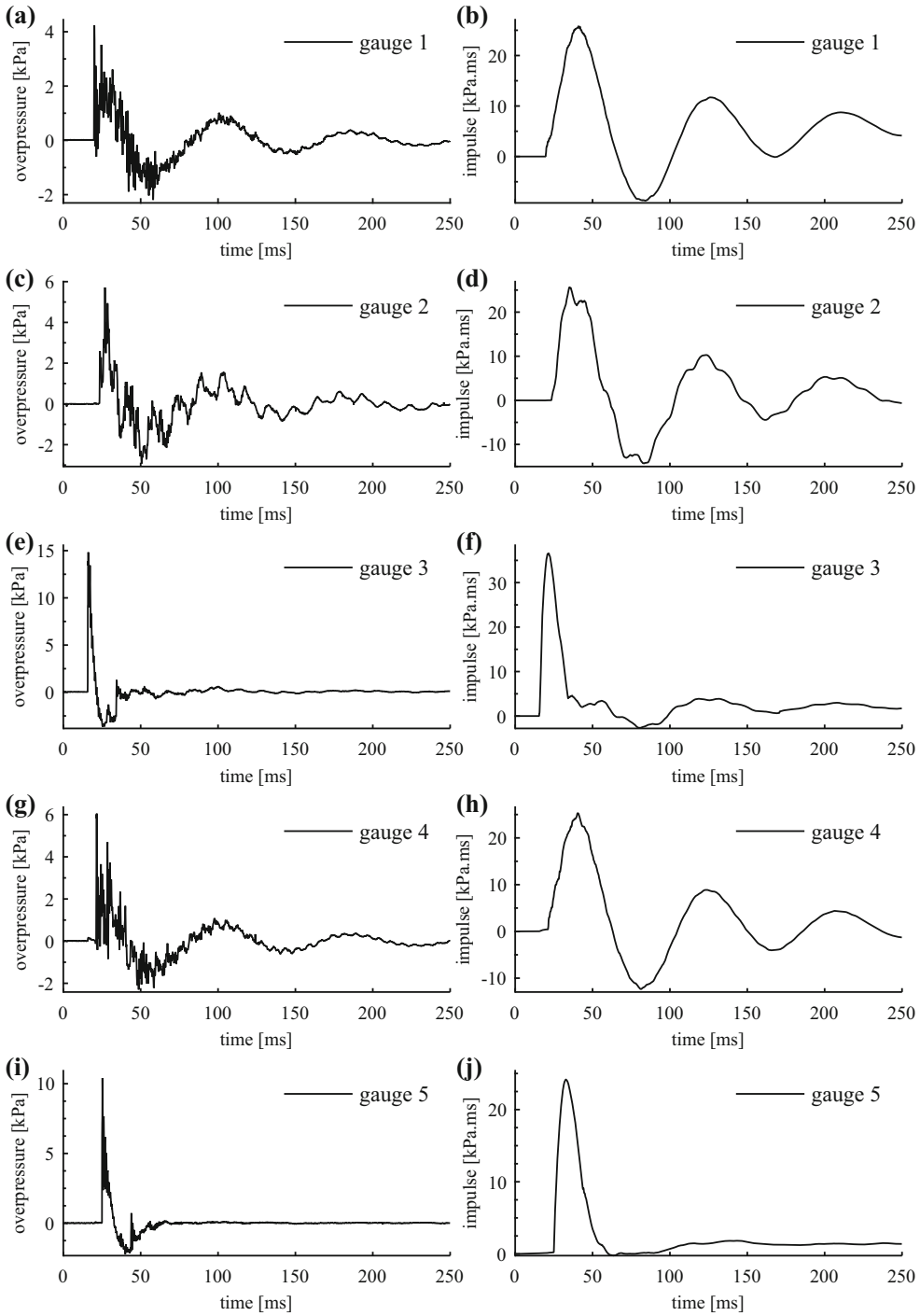

Fig. 6 Overpressure and impulse time history for test 3. **a**, **b** Center of the room. **c**, **d** Back wall. **e**, **f** Façade. **g**, **h** Side wall. **i**, **j** Exterior gauge

are compared with those computed using the empirical curves of UFC 3-340 [3]. This empirical method allows a good estimation of the maximum reflected overpressures inside and outside the room, but in some cases tends to underestimate the maximum values of reflected impulses. Finally, results of the dynamic response of the front masonry wall are presented in terms of accelerations and an iso-damage diagram.

2 Experimental setup

The field experiments were designed for studying a partially vented room exposed to different external blast loads. The blast tests were performed in a structure, designed and constructed for this series of tests of external explosions, as shown in Fig. 1. The structure was made of a reinforced concrete frame filled with four masonry walls. The room

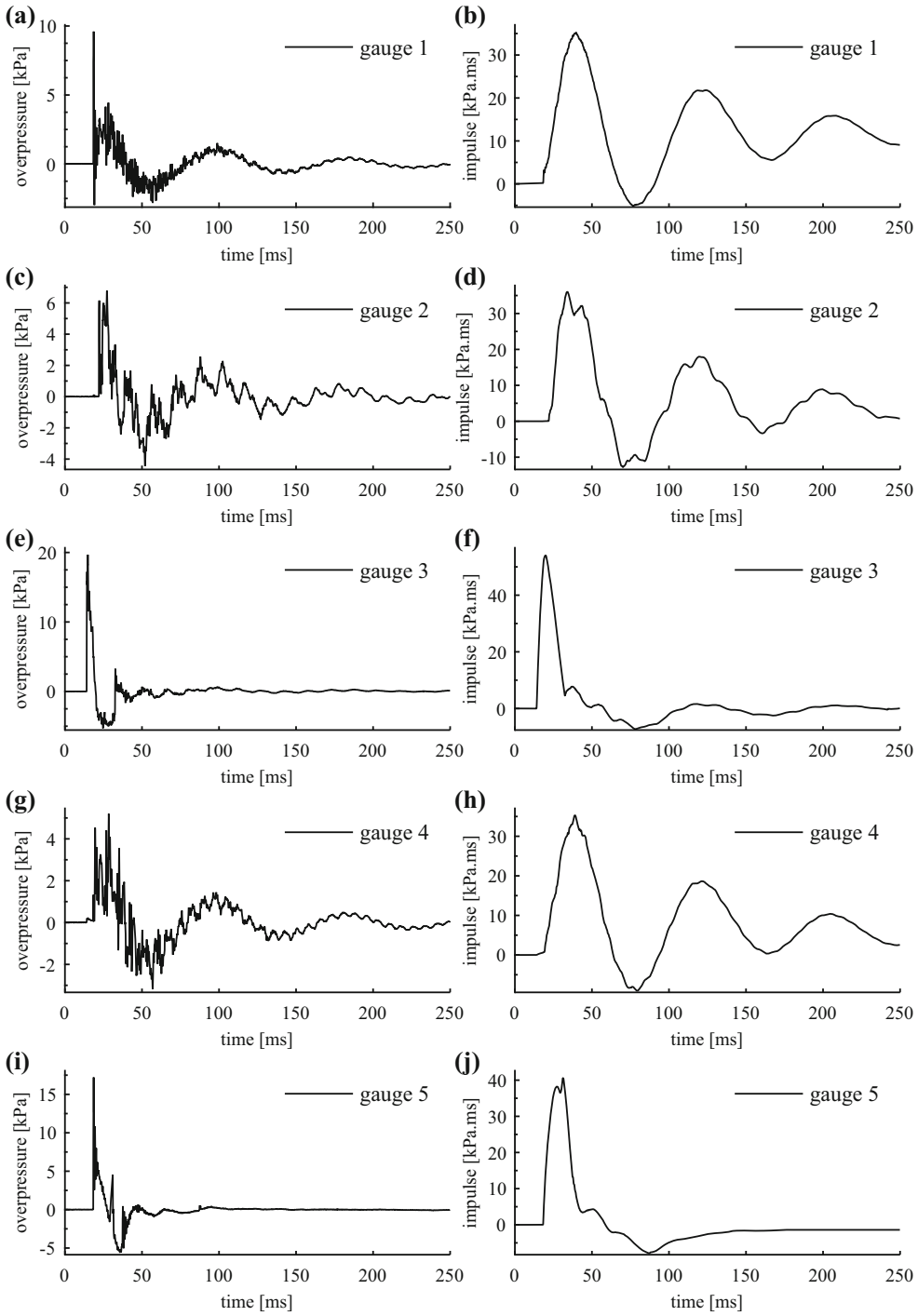

Fig. 7 Overpressure and impulse time history for test 4. **a**, **b** Center of the room. **c**, **d** Back wall. **e**, **f** Façade. **g**, **h** Side wall. **i**, **j** Exterior gauge

includes a square opening of 0.8 by 0.8 m in the front wall, and other dimensions are given in Figs. 1 and 2.

To measure the overpressures generated by the shock waves, five Honeywell 180PC pressure sensors were used, with locations shown in Fig. 2. Three sensors were installed inside the room (gauges 1, 2, and 4), and two outside (gauges 3 and 5). Gauge 3 was located under the opening to record the external blast wave reflection on the façade. The external blast wave was recorded by gauge 5. Inside the room, gauge 1 was placed in the center of the room, gauge 2 on the back wall, and gauge 4 on one of the sidewalls. To measure the structural response of the masonry, a PCB Piezotronics 352B01 accelerometer was used. The accelerometer was located in the inside face of the front wall (Fig. 2). A data acquisition

board (ComputerBoard PCM-DAS16D/16, 100 kHz bandwidth) was mounted in a notebook computer to record and process the signals by means of the program VEE 5.0. In all tests, the signals were sampled at a rate of 14,000 samples/s for each channel.

The explosive used for the tests was Gelamón VF65, consisting of a semi-plastic mass constituted by a gelatin of nitroglycerin-nitrocellulose with the incorporation of ammonia salts and several additives, equivalent in mass to 65% TNT. The properties of the explosive are presented in Table 1. Regarding the TNT equivalency of explosives, it is recognized that the level of variability is significant, typically 20–30% [24] and can be different for overpressures and impulses [24,25] and can also vary with the scaled distance [24]. However, the variability is higher in the near field and could be considered to be constant in the far field [24,26]. For these reasons, in Codina et al. [27] the equivalency of TNT, in terms of overpressures, was experimentally verified. All explosive charges were detonated using an electric initiation system with a detonator that was inserted into the bottom of the cylindrical charge. Table 2 shows the parameters for the four blast tests performed. Test 2 was repeated in test 4 to determine the degree of repeatability of the experimental method. The charge in test 3 had an angle of incidence of 30° with respect to the façade.

The scaled distance Z was defined in order to not far exceed the pressure range of the sensors (±2.5 psi). By definition, R is the distance in m from the focus of the explosion until the sensor G3 and W the mass of the explosive in kg of TNT. The explosive location for tests 1–4 is shown in plan in Fig. 3a. The height of burst in all tests was 1 m above the ground surface. The explosive load was suspended using a wood tripod (Fig. 3b). The atmospheric pressure recorded during the blast tests varied between 101.7 and 101.8 kPa, and the temperature varied between 14 and 16 °C.

Table 3 Maximum reflected overpressures (kPa)

Test	Gauge 1	Gauge 2	Gauge 3	Gauge 4	Gauge 5
1	7.68	5.26	14.54	3.38	14.25
2	9.05	6.45	18.41	4.78	16.61
3	4.23	5.71	14.83	6.05	10.40
4	9.60	6.77	19.69	5.19	17.21

Table 4 Maximum reflected impulses (kPa ms)

Test	Gauge 1	Gauge 2	Gauge 3	Gauge 4	Gauge 5
1	10.74	14.28	27.80	9.98	15.07
2	32.31	33.57	51.64	32.43	35.74
3	25.79	25.63	36.57	25.31	24.16
4	35.25	35.99	54.02	35.27	40.58

Table 5 Maximum reflected overpressures (kPa) for tests 2 and 4

Gauge	Test 2	Test 4	Dif. %
1	9.05	9.6	−6.1
2	6.45	6.77	−5.0
3	18.41	19.69	−7.0
4	4.78	5.19	−8.6
5	16.61	17.21	−3.6

Table 6 Maximum reflected impulses (kPa ms) for tests 2 and 4

Gauge	Test 2	Test 4	Dif. %
1	32.31	35.25	−9.1
2	33.57	35.99	−7.2
3	51.64	54.02	−4.6
4	32.43	35.27	−8.8
5	35.74	40.58	−13.5

3 Blast test results: overpressures and impulses

A total of four tests were carried out to investigate the leakage of the waves inside the partially vented room exposed to external explosions. The reflected overpressure and impulse time histories for tests 1–4 are presented in Figs. 4, 5, 6, and 7, respectively. The impulse time histories were obtained from numerical integration. The maximum impulse value is reached before 50 ms in all cases.

In all cases, the maximum reflected overpressures on the facade, gauge 3, were between two and three times higher than in the interior gauges (gauges 1, 2, and 4, Table 3). The maximum overpressure from gauge 1 (room center) was, on average, 44% of gauge 3 (façade). The maximum overpressure from gauge 2 (back wall) was, on average, 36% of gauge 3. Finally, the maximum overpressure from gauge 4 (side wall) was, on average, 29% of gauge 3. On the other hand, the maximum impulse reduction between the façade and interior gauges is lower than in the case of overpressures (Table 4). The maximum impulse from gauge 1 (room center) was, on average, 59% of gauge 3 (façade). The maximum impulse from gauge 2 (back wall) was, on average, 63% of gauge 3. Finally, the maximum impulse from gauge 4 (side wall) was, on average, 58% of gauge 3.

It is observed from tests 1–4, Figs. 4, 5, 6, and 7, that the impulse time histories from the interior gauges 1, 2, and 4 are rather similar. Furthermore, in all cases, the maximum reflected overpressures on gauge 5 (located outside the room, Fig. 2), were between two to three times higher than in the interior gauges (gauges 1, 2, and 4, Table 3). The maximum overpressure from gauge 1 (room center) was, on average, 51% of gauge 5 (exterior gauge). Considering that

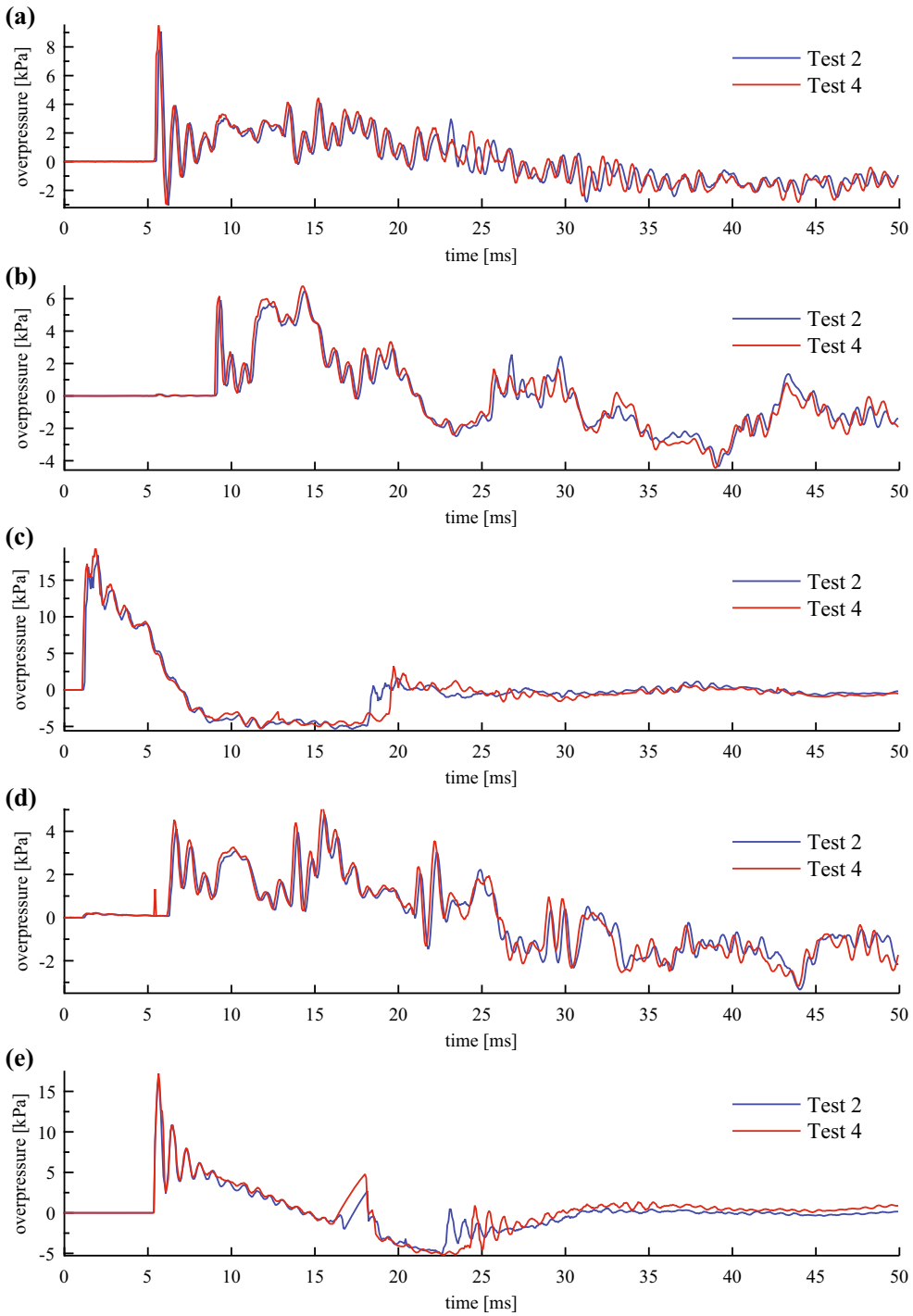

Fig. 8 Overpressure time history for test 2 and 4. **a** Center of the room. **b** Back wall. **c** Façade. **d** Side wall. **e** Exterior gauge

Table 7 Maximum reflected overpressures (kPa) for experimental tests and UFC prediction

Test	Gauge 2 (back wall)			Gauge 3 (façade)			Gauge 4 (side wall)		
	Test result	UFC	Dif. %	Test result	UFC	Dif. %	Test result	UFC	Dif. %
1	5.26	5.95	13.1	14.54	17.2	18.3	3.38	4.58	35.5
2–4[a]	6.61	6.188	−6.4	19.05	17.9	−6.0	4.985	5.65	13.3
3	5.71	5.093	−10.8	14.83	14.7	−0.9	6.05	4.68	−22.6

[a] Median value between test 2 and 4

Table 8 Maximum impulses (kPa ms) for experimental tests and UFC prediction

Test	Gauge 2 (back wall)			Gauge 3 (façade)			Gauge 4 (side wall)		
	Test result	UFC	Dif. %	Test result	UFC	Dif. %	Test result	UFC	Dif. %
1	14.28	13.22	−7.4	27.8	34.7	24.8	9.98	110	1002.2
2–4[a]	34.78	13.7	−60.6	52.83	67.2	27.2	33.85	169.2	399.9
3	25.63	11.43	−55.4	36.57	56.6	54.8	25.31	169.29	568.9

[a] Median value between the test 2 and 4

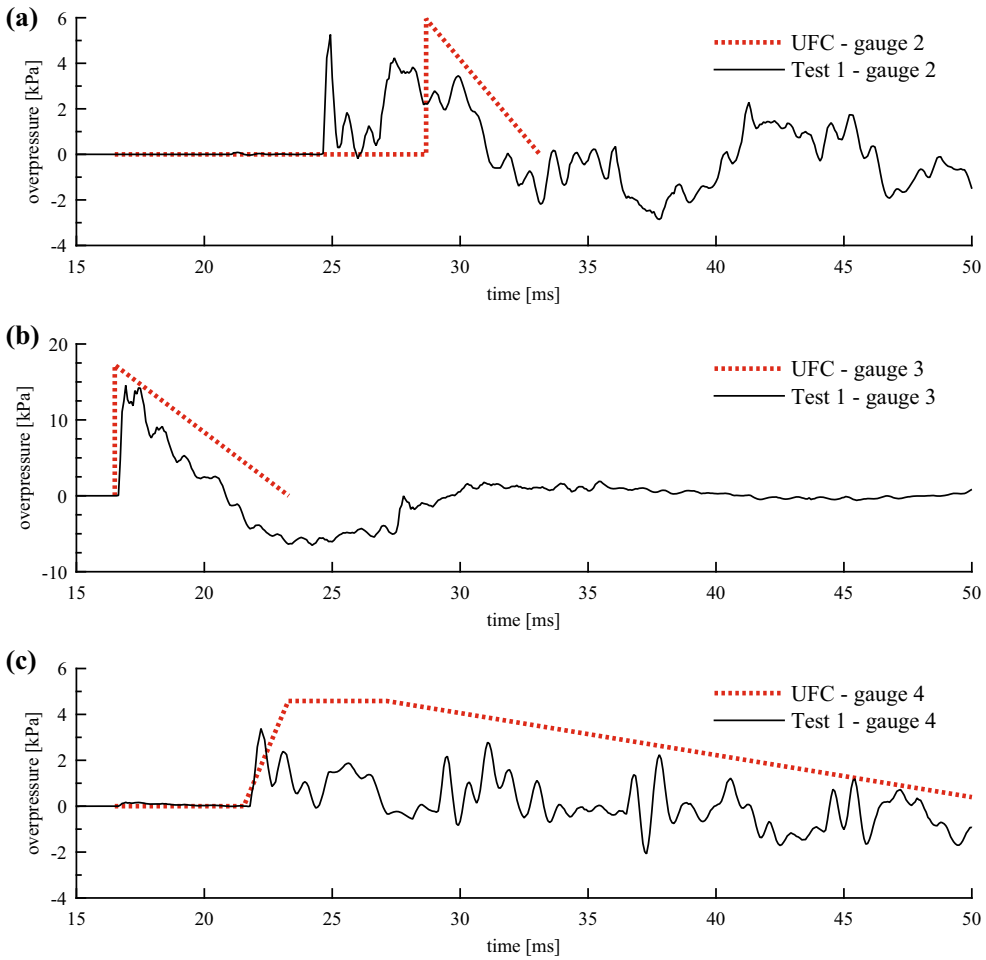

Fig. 9 Overpressures time histories for test 1 and UFC idealized pressure history. **a** Back wall. **b** Façade. **c** Side wall

both gauges are at the same distance R and, consequently, the same scaled distance Z, the differences should be attributed to the leakage of the blast waves. The maximum overpressure from gauge 2 (back wall) was, on average, 42% of gauge 5. Moreover, the maximum overpressure from gauge 4 (side wall) was, on average, 35% of gauge 5. On the other hand, the maximum impulse reduction between the exterior gauge and the interior gauges is lower than the case of overpressures (Table 4). The maximum impulse from gauge 1 (room center) was, on average, 88% of gauge 5 (exterior gauge). The maximum impulse from gauge 2 (back wall) was, on average, 95% of gauge 5. Finally, the maximum impulse from gauge 4 (side wall) was, on average, 87% of gauge 5. It is concluded that the multiple blast wave reflections and confinement inside the room significantly increase the impulse obtained.

3.1 Test repeatability

Test repeatability was also investigated, and significant variations among identical repeated tests were not observed. Table 5 presents the maximum overpressures recorded from tests 2 and 4. "Dif." is the relative difference, normalized with results of test 2. The differences observed are between −3.6 and −8.6%.

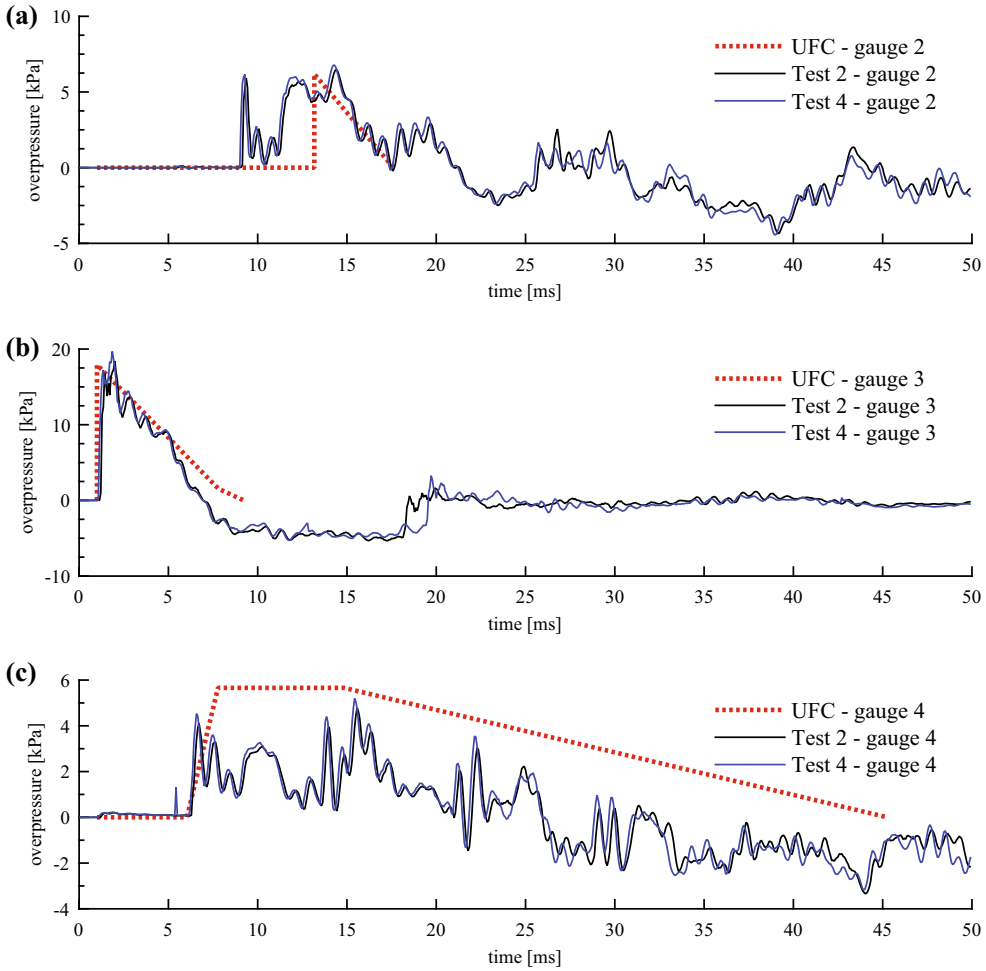

Fig. 10 Overpressures time histories for test 2, test 4, and UFC idealized pressure history. **a** Back wall. **b** Façade. **c** Side wall

In Table 6 are shown the maximum impulses recorded from tests 2 and 4. In that case, the differences observed are between −4.6 and −13.5%. The maximum reflected overpressures and impulses recorded in test 4 are slightly higher than in test 2 (Tables 5, 6).

Figure 8 presents the overpressure time histories for tests 2 and 4 for all gauges. It can be seen that both time histories are very similar. Hence, the repeatability of the tests may be reasonably confirmed.

3.2 UFC-3-340 method

Blast resistant design has been traditionally performed using idealized pressure and impulse loadings derived from empirical design charts provided in technical manuals such as the UFC 3-340 [3]. These empirical-analytical methods were developed thanks to massive research programs conducted since the beginning of the twentieth century. Among the numerous cases addressed in the UFC manual, one of them is the determination of idealized blast loads inside partially vented structures exposed to external blast loads. This method allows the estimation of blast arrival times over the internal walls, the maximum average overpressure on the walls, and the idealized times for the determination of the impulses. On the other hand, the UFC manual allows the determination of reflected overpressures over the façade and clearing times as a function of the façade geometry and opening size.

The experimental results of maximum reflected overpressure are compared in this section with those computed using the empirical curves of UFC 3-340 [3] (Table 7, in which "Dif." is the relative difference, normalized with test results). In the back wall, the differences between the experimental and computed results using the UFC 3-340 manual are −11 to 13%. On the other hand, in the façade the differences between the experimental and computed results are −6 to 18%. Finally, in the side wall the differences between the experimental and computed results are −23 to 35%.

The experimental results of maximum reflected impulses are compared with those computed using the empirical curves of UFC 3-340 [3] (Table 8, in which "Dif." is the relative difference, normalized with test results). In the back wall, the

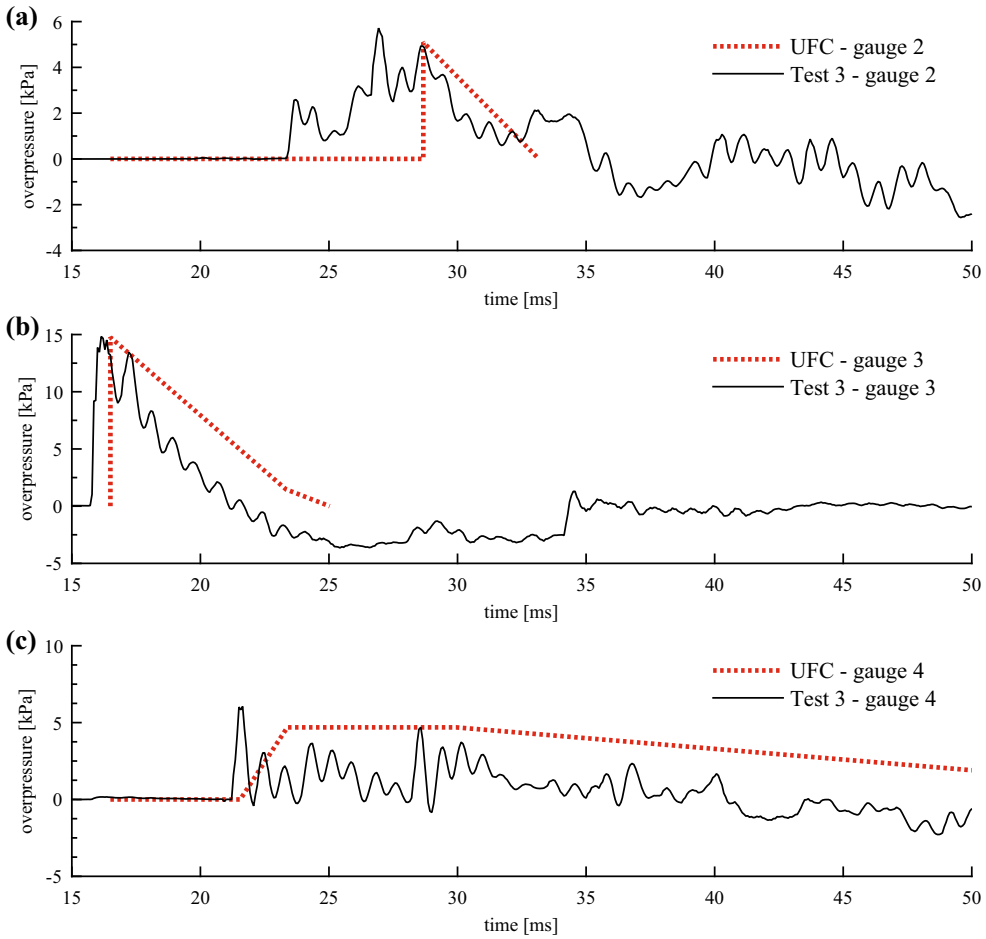

Fig. 11 Overpressures time histories for test 3 and UFC idealized pressure history. **a** Back wall. **b** Façade. **c** Side wall

differences between the experimental and computed results are −7 to −61%. In the back wall, the experimental values are higher in all cases. Otherwise, in the façade, the differences between the experimental and computed values are 25–55%. In the façade, the experimental values are lower in all cases. Finally, it is observed that the UFC method excessively overestimates the impulse on the side wall in the cases studied. In the side wall, the differences between the experimental and computed results are 400–1000%. In the side wall, the UFC 3-340 values are much higher in all cases.

It should be highlighted that some of the values obtained using the UFC 3-340 manual for the façade, back wall, and side wall, are near the limits of the figures. Hence, it can be inferred that the values obtained in the UFC 3-340 manual may have been obtained for higher explosive masses.

Figures 9, 10, and 11 present the overpressure time histories for tests 1–4, and the idealized overpressure time loads computed using the UFC 3-340 manual [3]. It can be seen that the arrival time to the side wall is correctly calculated using the UFC manual. In the case of the back wall, the arrival time exhibits a difference of 4 ms in test 1, 4.17 ms in tests 2 and 4, and 4.8 ms in test 3. In Figs. 9, 10, and 11 is shown that the experimental reflected overpressure in the façade exhibits a lower clearing time with respect to the UFC 3-340 prediction. This is because gauge 3 was located near to the bottom of the opening, which reduces the clearing times with respect to the overall clearing time on the façade.

Considering only the results on the façade and the clearing effects, it can be noted that the maximum reflected overpressures are well estimated by UFC 3-340 but the impulses are significantly overestimated. A similar conclusion was obtained by Tyas et al. [10], using experimental results with scaled distances similar to those used in this paper, and comparing the experimental results with those obtained by ConWep.

4 Structural response

The structural response is presented in terms of the acceleration records measured in the inside face of the front wall. The dynamic response of a masonry wall subjected to blast

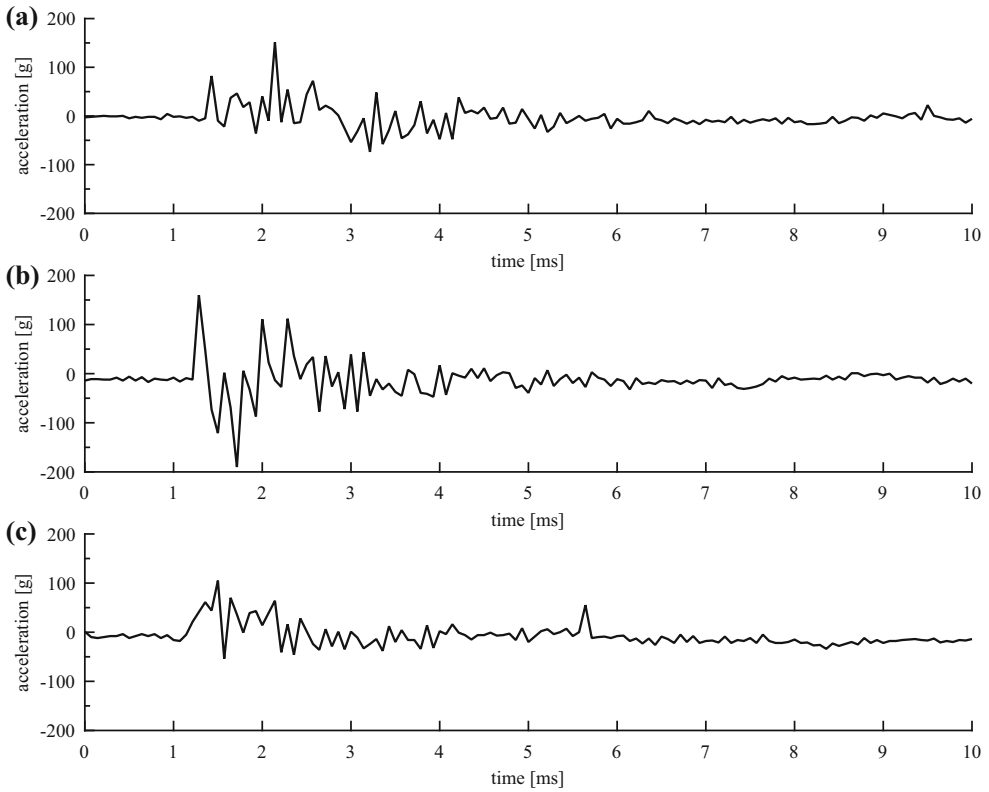

Fig. 12 Time history of accelerations recorded. **a** Test 1. **b** Test 2. **c** Test 3

Table 9 Recorded maximum accelerations

Test	Maximum accel. (g)
1	151.3
2	190.1
3	113.8

loading is a very difficult task for modeling due to different and variable nonlinear properties of mortar and bricks. The following experimental data are useful for checking the accuracy of a variety of calculation methods.

The accelerations obtained are presented in Fig. 12 and the maximum accelerations in Table 9. The result for test 4 could not be properly recorded due to problems with the accelerometer. The results of accelerations are consistent with the scaled distances for each test presented in Table 2.

In order to verify the behavior of the structure, the well-known iso-damage diagrams can be used. The chart presented by Millington [28], which relates incident overpressure to distance for different masses of explosive and damage levels, was used (Fig. 13). These curves correspond to explosive masses ranging from 1 to 500 kg of TNT and have a finer specification for damage levels in different types of structural and nonstructural elements. The iso-damage diagrams in terms of reflected pressures and impulses can be useful to obtain the levels of damage corresponding to reflected values of pressure and impulse obtained in the experimental tests.

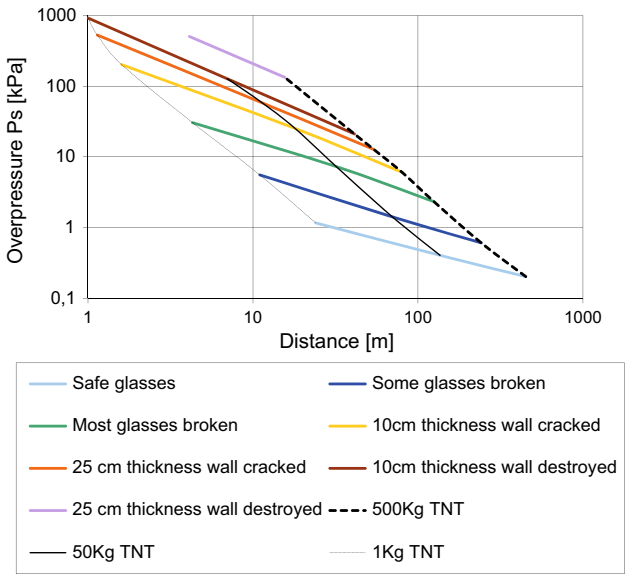

Fig. 13 Iso-damage curves by Millington [28]

These diagrams were also converted into graphics relating reflected values of pressure and impulse to damage levels by Luccioni et al. [29] and Ambrosini et al. [30]. The results for gauge G3 (front wall) and for the four tests are presented in Fig. 14. The points for the four tests are near the curve

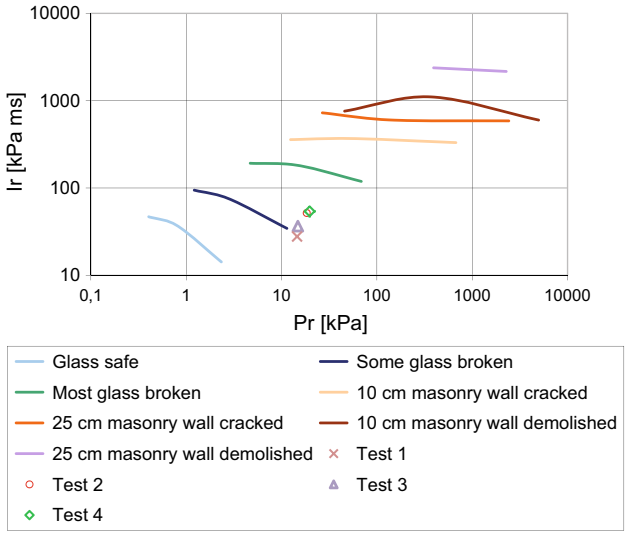

Fig. 14 Response of the structure

denoted "Some glass broken" and below the curve "10 cm masonry wall cracked" which is consistent with the lack of damage to the wall observed after the blasts.

5 Conclusions

A full-scale experimental test was presented with the aim of studying the effect of leakage of the blast waves inside a partially vented room subjected to external explosions. Three explosions with different charges and scaled distances were used. A fourth blast was used to examine the repeatability of the results. The results presented are useful for determining the validity of different methods of calculation, both empirical and numerical.

Overpressures and impulse time histories from pressure gauges located at different points inside and outside the room were analyzed. In all cases, the maximum reflected overpressure on the façade (gauge 3) was between two and three times higher than in the interior gauges. Otherwise, the maximum impulse reduction between the exterior gauge and the interior gauges was lower than the overpressures. It is concluded that the multiple blast wave reflections inside the room and confinement significantly increase the impulse obtained. In addition, the impulse time histories from the interior, back wall, side wall and center of the room gauges were rather similar.

Test repeatability was also investigated in tests 1 and 4. In the case of the maximum reflected overpressures, the differences observed are between 3.6 and 8.6%. For maximum reflected impulses, the observed differences are between 4.6 and 13%. Moreover, the time histories of both tests are rather similar. Hence, the repeatability of the results has been reasonably confirmed.

The experimental results were compared with those computed using the empirical curves of UFC 3-340 [3]. This empirical method allows a good estimation of the maximum reflected overpressures inside and outside the room. The UFC 3-340 method tends to significantly overestimate the impulse in the side wall. On the other hand, this method tends to underestimate the impulse on the back wall, and so in this case the UFC method does not predict a conservative value. In the case of the façade, it was observed that the UFC 3-340 method predicts impulse values between 25 and 55% greater than in the tests. The reason is that the experimental reflected overpressures in the facade exhibit a lower clearing time with respect to the UFC 3-340 prediction. This is because gauge 3 was located near to the bottom of the opening, which reduces the clearing times with respect to the overall clearing time on the façade. The shock arrival time at the side wall is correctly calculated using the UFC manual, although for the case of the back wall, the predicted arrival time exhibits some differences from the experimental observations.

The previous conclusions about the accuracy of the empirical UFC 3-340 method are valid within the pressure range and charge weights employed in the tests.

Finally, regarding the dynamic response of the front masonry wall, large accelerations were measured, up to a value of 190 g. On the other hand, a very short time response was measured of about 2.5 ms. Considering the overpressures and impulses measured and the location on the iso-damage diagram, it can be concluded that the dynamic response of the front masonry wall was linear elastic, as expected.

Acknowledgements The cooperation in the blast tests of Oscar Curadelli, Gabriel Houri, Fernanda de Borbón, Martín Domizio, Hernán Garrido, and Carlos Martínez are specially acknowledged. The financial support of CONICET (Argentina) and SECTYP (National University of Cuyo) is also gratefully acknowledged. Special acknowledgements are extended to the reviewers of the first version of the paper because their useful suggestions led to improvements of the work.

References

1. Goel, M.D., Matsagar, V.A.: Blast-resistant design of structures. Pract. Period. Struct. Des. Constr. **19**, 4014007 (2014). doi:10.1061/(ASCE)SC.1943-5576.0000188
2. van der Voort, M.M., van Wees, R.M.M., Brouwer, S.D., van der Jagt-Deutekom, M.J., Verreault, J.: Forensic analysis of explosions: Inverse calculation of the charge mass. Forensic Sci. Int. **252**, 11–21 (2015). doi:10.1016/j.forsciint.2015.04.014
3. U.S. DoD: Structures to Resist the Effects of Accidental Explosions. Deparment of Defense, Washington, DC, USA. UFC 3-340-02 (2008)
4. U.A.E.W.E. Station: Fundamentals of Protective Design for Conventional Weapons. TM5-855-1, Department of the Army, Vicksburg (1986)

5. U.S. Army En: ConWep, Conventional Weapons Effects Program. D.W. Hyde, US Army En, Vicksburg (1991)
6. Baker, W.E., Cox, P.A., Westine, P.S., Kulesz, J.J., Strehlow, R.A.: Explosion Hazards and Evaluation. Elsevier, Amsterdam (1983)
7. Smith, P.D., Hetherington, J.G.: Blast and Ballistic Loading of Structures. Butterworth-Heinemann, Oxford, Great Britain (1994)
8. Cormie, D., Mays, G., Smith, P.: Blast Effects on Buildings, 2nd edn. Thomas Telford Ltd, London (2009)
9. Smith, P.D., Rose, T.A., Krahe, S.L., Franks, M.A.: Façade failure effects on blast propagation along city streets. Proc. Inst. Civ. Eng. Struct. Build. **156**, 359–365 (2003). doi:10.1680/stbu.2003.156.4.359
10. Tyas, A., Warren, J.A., Bennett, T., Fay, S.: Prediction of clearing effects in far-field blast loading of finite targets. Shock Waves **21**, 111–119 (2011). doi:10.1007/s00193-011-0308-0
11. Wang, X., Remotigue, M., Arnoldus, Q., Janus, M., Luke, E., Thompson, D., Weed, R., Bessette, G.: High-fidelity simulations of blast loadings in urban environments using an overset meshing strategy. Shock Waves **27**, 409–422 (2017). doi:10.1007/s00193-016-0680-x
12. Rose, T.A., Smith, P.D., May, J.H.: The interaction of oblique blast waves with buildings. Shock Waves **16**, 35–44 (2006). doi:10.1007/s00193-006-0051-0
13. Remennikov, A.M., Rose, T.A.: Modelling blast loads on buildings in complex city geometries. Comput. Struct. **83**, 2197–2205 (2005). doi:10.1016/j.compstruc.2005.04.003
14. Smith, P.D., Rose, T.A.: Blast wave propagation in city streets—an overview. Prog. Struct. Eng. Mater. **8**, 16–28 (2006). doi:10.1002/pse.209
15. Luccioni, B., Ambrosini, D., Danesi, R.: Blast load assessment using hydrocodes. Eng. Struct. **28**, 1736–1744 (2006). doi:10.1016/j.engstruct.2006.02.016
16. Gebbeken, N., Döge, T.: Explosion protection—Architectural design, urban planning and landscape planning. Int. J. Prot. Struct. **1**, 1–22 (2010). doi:10.1260/2041-4196.1.1.1
17. Codina, R., Ambrosini, D., de Borbón, F.: Numerical study of confined explosions in urban environments. Int. J. Prot. Struct. **4**, 591–617 (2013). doi:10.1260/2041-4196.4.4.591
18. Feldgun, V.R., Karinski, Y.S., Edri, I., Yankelevsky, D.Z.: Prediction of the quasi-static pressure in confined and partially confined explosions and its application to blast response simulation of flexible structures. Int. J. Impact Eng. **90**, 46–60 (2016). doi:10.1016/j.ijimpeng.2015.12.001
19. Anderson, C.E., Baker, W.E., Wauters, D.K., Morris, B.L.: Quasi-static pressure, duration, and impulse for explosions (e.g. HE) in structures. Int. J. Mech. Sci. **25**, 455–464 (1983). doi:10.1016/0020-7403(83)90059-0
20. Edri, I., Savir, Z., Feldgun, V., Karinski, Y., Yankelevsky, D.: On blast pressure analysis due to a partially confined explosion: I. Experimental studies. Int. J. Prot. Struct. **2**, 1–20 (2011). doi:10.1260/2041-4196.2.1.1
21. Sauvan, P.E., Sochet, I., Trélat, S.: Analysis of reflected blast wave pressure profiles in a confined room. Shock Waves **22**, 253–264 (2012). doi:10.1007/s00193-012-0363-1
22. Ram, O., Nof, E., Sadot, O.: Dependence of the blast load penetrating into a structure on initial conditions and internal geometry. Exp. Therm. Fluid Sci. **78**, 65–74 (2016). doi:10.1016/j.expthermflusci.2016.05.012
23. Luccioni, B., Ambrosini, D., Danesi, R.: Analysis of building collapse under blast loads. Eng. Struct. **26**(1), 63–71 (2004). doi:10.1016/j.engstruct.2003.08.011
24. Locking, P.: The trouble with TNT equivalence. In: 26th International Symposium on Ballistics, Miami, FL, 12–16 September (2011)
25. Locking, P.: TNT equivalence—experimental comparison against prediction. In: 27th International Symposium on Ballistics, Freiburg, 22–26 April (2013)
26. Grisaro, H., Edri, I.: Numerical investigation of explosive bare charge equivalent weight. Int. J. Prot. Struct. **8**, 199–220 (2017). doi:10.1177/2041419617700256
27. Codina, R., Ambrosini, D., de Borbón, F.: Alternatives to prevent the failure of RC members under close-in blast loadings. Eng. Fail. Anal. **60**, 96–106 (2016). doi:10.1016/j.engfailanal.2015.11.038
28. Millington, G.: Discussion of 'The protection of buildings against terrorism and disorder'. In: Elliott, C.L., Mays, G.C., Smith, P.D. (eds.) Proceedings of the Institution of Civil Engineers-Structures & Buildings, vol. 104, pp. 343–346 (1994)
29. Luccioni, B., Ambrosini, D., Danesi, R.: Analysing explosive damage in an urban environment. Proc. Inst. Civ. Eng. Struct. Build. **158**, 1–12 (2005). doi:10.1680/stbu.2005.158.1.1
30. Ambrosini, D., Luccioni, B., Jacinto, A., Danesi, R.: Location and mass of explosive from structural damage. Eng. Struct. **27**, 167–176 (2005). doi:10.1016/j.engstruct.2004.09.003